

Geometrical structure of benzene absorbed on Si(001)

U. Birkenheuer *, U. Gutdeutsch, N. Rösch

Lehrstuhl für Theoretische Chemie, Technische Universität München, 85747 Garching, Germany

Received 25 September 1997; accepted for publication 16 February 1998

Abstract

Although many details are known from experiments about the adsorption of benzene on Si(001), no definite structural proposal has so far been derived. Thus, “first principles” density functional energy optimizations have been performed for various structure models which were chosen in accordance with available experimental information on $C_6H_6/Si(001)$. By means of symmetry-resolved projected densities of states, the photoemission spectrum of benzene on Si(001) is simulated and analyzed according to dipole selection rules for each of the structure models. In addition, the vibrational properties of the various adsorption complexes are calculated using cluster models and the character of the vibrational modes is determined. The various structure models exhibit several distinct differences in electronic and vibrational properties. By comparison to experimental photoemission and energy-loss spectra of $C_6H_6/Si(001)$, the structure of the adsorption complex is derived, a C_{2v} symmetric 1,4-cyclohexadiene-like adsorption complex with a flat-lying benzene molecule, di- σ bound to one silicon surface dimer. This is consistent with the results of “first principles” geometry optimizations. Furthermore, based on this structure model, a rationalization of the unexpected (2×1) electron diffraction pattern observed for $C_6H_6/Si(001)$ at a saturation coverage of 1/4 ML is given. © 1998 Elsevier Science B.V. All rights reserved.

Keywords: Aromatics; Chemisorption; Density functional calculations; Excitation spectra calculations; Low index single crystal surfaces; Photoelectron emission; Silicon; Vibrations of adsorbed molecules

1. Introduction

The adsorption of hydrocarbons on silicon surfaces has been the topic of many recent investigations. Due to a large number of experimental (e.g. Refs. [1–4]) and theoretical studies (e.g. Refs. [4–8]), the basic bonding mechanism of unsaturated hydrocarbons is now well understood, although details of the geometrical structure of the adsorption complexes are still subject to discussion [3,6,8]. Far less is known about the interaction of

aromatic hydrocarbons with the (001) surface of silicon.

The first insight into the chemisorption of benzene on Si(001) was provided by the experimental investigation of Taguchi et al. [9]. From thermal desorption measurements (TDS) and Auger electron intensities (AES), they concluded that benzene is chemisorbed non-dissociatively with a saturation coverage of about 0.27 ML, which corresponds to one adsorbate per two surface Si dimers. Low-energy electron diffraction (LEED) at 300 and 90 K shows a (2×1) pattern with slightly increased background intensity [9] which seems to contradict the quarter monolayer saturation coverage deduced from AES and TDS data.

* Corresponding author.
E-mail: birken@theochem.tu-muenchen.de

High-resolution electron energy-loss spectroscopy (HREELS) [9] reveals substantial rehybridization within the benzene molecule upon chemisorption: sp^2 as well as sp^3 hybridized carbon atoms are present in the adsorption complex, indicating the formation of covalent σ bonds towards the silicon substrate. In addition, a signal at 1635 cm^{-1} , characteristic of C=C double bonds, was found in the EELS spectrum. Based on these results, two structure models with two C=C double bonds were proposed [9], a 1,3- and a 1,4-cyclohexadiene-like structure, each di- σ bound to the substrate. Possible realizations of such structures are shown in Fig. 1b and c.

These experimental results stimulated two theoretical investigations aiming at a more detailed structural description of the adsorption system $C_6H_6/Si(001)$ [10,11]. Both studies employed a semiempirical approach to the electronic structure and total energy of the adsorption system. In Ref. [10] the MINDO method was used, and the substrate was modeled by a slab of six Si layers: the silicon surface dimers and all atoms in the subjacent three substrate layers were allowed to relax. On the other hand, Jeong et al. [11] performed calculations with the PM3 method, using

a large $Si_{43}H_{32}$ cluster to describe the Si(001) substrate. They imposed several geometrical constraints during the geometry optimization [11], the most severe of them being fixed positions of the Si dimer atoms. The energetically favored structure found in the slab model study [10] corresponds to a tilted cyclohexene-like adsorbate (with only one C=C bond), four-fold σ -bound to a single Si surface dimer, with the dimer bond being broken (not shown in Fig. 1). The equilibrium structure resulting from a 1,4-cyclohexadiene-like starting configuration similar to that of Fig. 1b, but with the benzene molecule above the troughs of the reconstructed Si(001) surface was found to be less stable by 1.97 eV. Unfortunately, the corresponding structure on top of the Si dimer rows (Fig. 1b) was not considered. According to the PM3 calculations [11], a pedestal-like structure as shown in Fig. 1a, but slightly distorted, is the minimum-energy configuration of the adsorption system $C_6H_6/Si(001)$. However, no carbon double bonds exist in this structure, although some of the C–C bond lengths were computed to be 1.40 \AA , which is the C–C bond distance of benzene. Starting from the optimized geometry predicted by Craig [10], a metastable 1,3-cyclohexadiene-like struc-

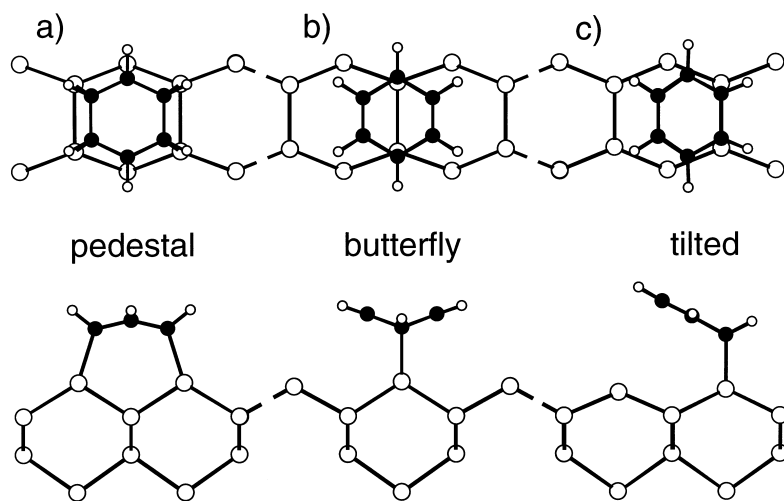


Fig. 1. Various structure models for the adsorption complex $C_6H_6/Si(001)$ viewed perpendicular to the surface (upper panel) and along the silicon surface dimers (lower panel). Shown are the equilibrium geometries of the model clusters employed for each structure as resulting from the DF total energy minimization (“pedestal” and “butterfly” structures) or the MINDO/d optimization (tilted structure). Hydrogen atoms saturating dangling bonds are not shown.

ture (Fig. 1c) consistent with the experimental results [9] was found, 0.29 eV higher in energy than the pedestal-like structure [11]. In line with the findings of the MINDO study [10], adsorption above the Si(001)-(2 × 1) troughs turned out to be disfavored by 1.2–1.5 eV. The differences in the semiempirical methods employed may be one reason for the prediction of different minimum-energy structures: the different descriptions of the Si dimers may be another. On the other hand, the alternative substrate models (slab and cluster) should be less likely reasons for the calculated differences. However, Craig [10] did not consider a pedestal-like structure at all: therefore, such an adsorption structure cannot be ruled out to represent the lowest total-energy configuration within the MINDO approach as well. Unfortunately, only bonding energies were reported in these two studies [10,11]. Thus, a direct comparison to the experiments [9] is not possible.

Obviously, further investigations are necessary to clarify the geometrical structure of the adsorption system C₆H₆/Si(001). To reach this goal, a combined approach employing both experimental and theoretical results is used. Based on the measurements of Taguchi et al. [9] and recent angle-resolved ultraviolet photoemission spectroscopy (ARUPS) data [12], two structure models are proposed. By means of “first principles” density functional (DF) cluster calculations, the equilibrium configurations of these two structure models have been determined. From a comparison of the corresponding binding energies, a first indication of the geometrical structure of the adsorption system is obtained. However, for a definitive discrimination, the electronic and vibrational properties of the two structure models have been simulated: they exhibit several significant differences. Thus, by direct comparison to the photoemission and energy-loss spectra now available for the adsorption system C₆H₆/Si(001), a conclusive structural proposal is derived which also offers a consistent rationalization for the unexpected observed (2 × 1) LEED pattern [9].

2. Computational details

Benzene is non-dissociatively σ -bound to Si(001)-(2 × 1) [9] and, according to recent photo-

emission data [12], the local symmetry of the adsorption complex is C_{2v}, with the molecular plane oriented parallel to the surface. Tilted adsorption complexes such as the 1,3-cyclohexadiene-like complex in Fig. 1c or the minimum total-energy configuration found in Ref. [10] are not compatible with these findings. Furthermore, the formation of adsorption complexes bridging the troughs of the (2 × 1) reconstructed should be energetically disfavored with respect to adsorption on top of the dimer rows because two unsaturated Si surface atoms would remain after chemisorption in this case (at least in the initial low-coverage state of the process). This reasoning is supported by previous semiempirical calculations [10,11] where all bridging adsorption complexes considered were found to be less stable than the corresponding on-top configurations by at least 1.2 eV. We therefore focus on adsorption above the dimer rows of the reconstructed Si(001) surface. There exist several realizations of such adsorption complexes with a flat-lying, σ -bound benzene molecules which are compatible with the experimentally observed C_{2v} symmetry, but only two of them result in “chemically reasonable” bonding configurations. One realization is the four-fold bound structure shown in Fig. 1a, which will be called “pedestal” in the following. The other, hereafter denoted “butterfly” structure, is the 1,4-cyclohexadiene-like adsorption complex mentioned above [9] (Fig. 1b). These two structure models are quite distinct with respect to their geometrical as well as their electronic configuration. The “butterfly” structure represents a closed-shell system with two C=C double bonds and two sp³ hybridized carbon atoms which form the Si–C bonds. The “pedestal” structure is a biradical, open-shell system with a localized p_z-type electron on each of the two sp² hybridized carbon atoms not involved in the Si–C bonds. At first glance, such a radical structure of the adsorbed benzene seems to be unfavorable compared to the 1,4-cyclohexadiene-like structure, but one has to consider that in this way each adsorbate is able to saturate two pairs instead of only one pair of Si dimer dangling bonds. More quantitatively, the stability of potential adsorption complexes can be estimated by comparing the bond formation ener-

gies gained to the energies required in order to prepare the adsorbate and the substrate for bonding (see Section 3.1).

The substrate cluster models employed in the present investigation are chosen such that they comprise (i) those surface dimer silicon atoms directly bound to the adsorbate, (ii) all nearest-neighbor substrate atoms of those dimer atoms, and (iii) all atoms of the Si(001) substrate which are at least two-fold coordinated to the central cluster set up in steps (i) and (ii). To account for a possible interaction between hydrogen atoms of benzene and unsaturated Si dimers, the cluster model for the “butterfly” structure is augmented by one surface silicon dimer on each side of the interacting dimer. The resulting substrate clusters for “pedestal” and “butterfly” adsorption, $\text{Si}_{15}\text{H}_{16}$ and $\text{Si}_{13}\text{H}_{12}$, respectively, are shown in Fig. 1. The dangling bonds toward the substrate are saturated by hydrogen atoms with a Si–H distance of 1.48 Å, as found in SiH_4 [13]. Structural relaxation is allowed for the adsorbate and for the active surface Si dimer, while the subsurface Si atoms of the model clusters are fixed to positions obtained from a bulk-terminated geometry (with a lattice constant of 5.43 Å [14]). The geometry of the unsaturated Si dimers added to the model cluster of the “butterfly” structure is taken from a reference model cluster calculation on the clean reconstructed Si(001)-(2 × 1) surface.

Geometry optimization was carried out in two steps. First, the adsorption complex was optimized by means of semiempirical total energy and force calculations. Local C_{2v} symmetry was found both for the “pedestal” and the “butterfly” structures. These equilibrium structures were then taken as starting configurations for the final “first principles” DF geometry optimization, where a C_{2v} symmetry of the adsorption complex was imposed. As a rule, binding energies are quoted here as differences in total energies between the equilibrium structure of the modeled adsorption complex and its individually geometry-optimized constituents, e.g. the corresponding “naked” substrate cluster and the isolated adsorbate: exceptions to this will be indicated explicitly.

The semiempirical calculations on the cluster

models were performed with the MNDO/d method [15] as implemented in the program SIBIQ [16]. For Si, the recently developed parametrization including d orbitals [17] was used. The “first principles” DF calculations were carried out with the LCGTO-DF program (linear combinations of Gaussian-type orbitals; density functional) [18]. Gradient-corrected exchange energy [19] and correlation energy functionals [20] were used during the Kohn–Sham SCF (self-consistent field) procedure for determining the charge density as well as for the evaluation of the total energy and the corresponding analytical displacement derivatives. A numerical integration scheme [21,22] was employed to compute quantities related to the exchange-correlation energy. The orbital basis set for Si was generated by contracting a (12s,9p,2d) basis set to [6s,4p,2d] using atomic eigenvectors. The (9s,5p,1d) → [4s,3p,1d] basis set for C and the (6s,1p) → [3s,1p] basis sets for H were set up in the same way. The uncontracted basis sets were taken from previous investigations of zeolites [23] (Si) and adsorption of hydrocarbons on transition metal surfaces [24–26] (C and H). Test calculations showed that these orbital basis sets are well suited to predicting the properties of organo-silicon compounds like SiH_4 and H_3SiCH_3 . In the LCGTO-DF method, auxiliary basis set are employed to represent the electron charge density. s- and r^2 -type charge fitting functions were chosen in the standard fashion [27], i.e. by scaling the s- and p-type exponents, respectively, of the orbital basis functions by a factor of two. Furthermore, for each atom the fitting basis sets were augmented by p-type polarization functions with exponents of 0.1, 0.25, 0.625, 1.5625, and 3.90625 au [27]; d-type polarization functions with exponents twice as large were added to the fitting basis sets of the “heavy” atoms C and Si.

3. Results and discussion

3.1. The geometrical structure

If the RHF (restricted Hartree–Fock) approximation is applied to optimize the substrate model

clusters $\text{Si}_{13}\text{H}_{12}$ and $\text{Si}_{15}\text{H}_{16}$ without the adsorbate, the MNDO/d method yields buckled surface Si dimers for both clusters. A polarized π -bond between the Si atoms of the surface dimers is formed in this case, in agreement with the commonly accepted picture of the reconstructed Si(001) surface, and as predicted by many DF calculations (see, e.g., Ref. [28], and references therein). If, however, the UHF (unrestricted Hartree–Fock) approximation is employed (with the total spin difference fixed to zero), equilibrium structures with symmetric Si dimers are found which are considerably lower in energy (by 0.4–0.8 eV) than the corresponding RHF minimal total-energy configurations. Electron localization (which is not possible in the RHF description) is the driving force for the observed change in the geometry. Instead of forming a π -bond, two localized electrons with anti-parallel spin reside in the dangling bonds of the surface dimers. These findings are in line with the results of a recent *ab initio* Hartree–Fock model cluster investigation of the Si(001) surface [29]. Thus, all further semiempirical calculations have been performed in an unrestricted fashion.

In all cases, the singlet-type UHF state with a vanishing z -component of the total spin turned out to be the ground state. The corresponding binding energies for the adsorption of benzene on Si(001) amount to 2.3 and 3.3 eV for the “butterfly” and “pedestal” structures, respectively. Hence, within the MNDO/d approach the four-fold bound “pedestal” structure is energetically favored, in line with the semiempirical PM3 study of Jeong et al. [11]. Highly localized electrons are found on the two three-fold coordinated carbon atoms of the biradical “pedestal” structure. No significant direct interaction is expected between these two electrons: the electronic configurations with parallel and anti-parallel spin of the two radical electrons are almost degenerate (splitting of 6 meV). No geometry constraint was imposed during this pre-optimization, yet the equilibrium configurations of the two structure models exhibit local C_{2v} symmetry. Thus, these configurations correspond to local minima of the energy surface of the corresponding model cluster. In this sense,

the MNDO/d calculations confirm the C_{2v} symmetry derived from the photoemission data [12].

The “first principles” DF calculations of the structure models for benzene adsorbed on Si(001) have been performed in two ways: spin-restricted as well as spin-polarized (with the spins of all unpaired electrons parallel to avoid symmetry-breaking due to spin localization). At the initial geometries of the “naked” substrate model clusters prior to benzene adsorption, the spin-restricted ground states are found to be substantially lower in energy (by about 1 eV) than the corresponding spin-polarized electronic structures, even though the stabilizing dimer buckling is missing here. Hence, the electronic ground-state configurations exhibit a doubly occupied (covalent) π -bond orbital along the Si dimer which is formed by two weakly overlapping p_z -type dangling bonds at the Si surface atoms rather than two single occupied dangling-bond states or their symmetry-adapted π - and π^* -like counterparts. Obviously, DF calculations favor the more covalent one-electron picture of the surface Si dimers as compared to the semi-empirical (see above) or pure Hartree–Fock description [29], a general trend which has also been observed for ionic systems [30]. The DF optimization for the “butterfly” complex, both substrate clusters and the isolated adsorbate, has therefore been carried out in spin-restricted fashion. Only for the “pedestal” adsorption complex, which is clearly a biradical, have spin-polarized calculations been performed. In fact, at the starting geometry, the spin-polarized ground state of this structure was found to be 0.42 eV more stable than the spin-restricted ground state. Electron localization (as confirmed by a Mulliken population analysis) takes place, and the level splitting between the “bonding” and “anti-bonding” linear combination of the p_z orbitals on the two separated carbons atoms amounts to 0.18–0.19 eV only (for α and β spin; see Fig. 2b), providing further evidence for a rather small spatial overlap of these two orbitals.

The most striking result of the “first principles” geometry optimizations, however, is that the energetic ordering of the adsorption models is opposite to that predicted by the semiempirical calculations.

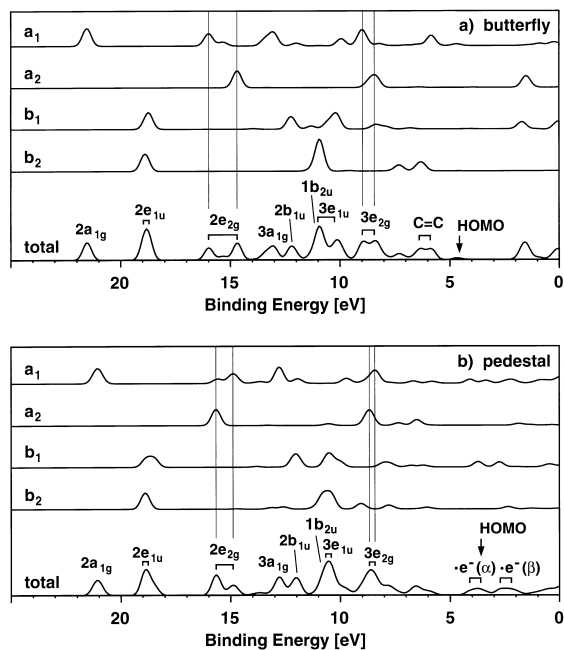


Fig. 2. Density of states (DOS) of the Kohn–Sham one-particle energies calculated for the “butterfly” and the “pedestal” model clusters, total DOS (lower part) as well as symmetry-resolved DOS according to the irreducible representations of symmetry group C_{2v} (upper part), all weighted by the Mulliken populations on the adsorbate. States originating from the benzene σ system are labeled accordingly. Also marked are the C=C double-bond states of the “butterfly” structure, the occupied and virtual states describing the radical electrons of the “pedestal” structure, and the HOMO energy of each model cluster.

With a binding energy of 1.40 eV the “butterfly” structure is now strongly favored over to the “pedestal” structure, whose binding energy amounts to only 0.15 eV. Taking into account a dimer buckling energy of 0.14 eV [31] for each Si dimer involved in the chemisorption process, an energy difference between the two adsorption models of 1.39 eV is found. Binding energies obtained from model cluster calculations should be interpreted with due caution since cluster size convergence of this property is known to be rather slow [32,33]. Thus, an overall uncertainty of a few tenths of an eV remains. However, the computed energy difference is much larger. Yet, independent evidence discriminating the two structure models

is desirable, and indeed will be given in the following sections.

The geometrical details of the 1,4-cyclohexadiene-like equilibrium structure of the adsorption complex are summarized in Table 1 for both the semiempirical MNDO/d pre-optimization and the final “first principles” DF optimization. Overall, the results of the two methodologies are quite similar, especially for the adsorbate, as was to be expected since semiempirical schemes are considered to be rather reliable for organic compounds. On the other hand, deviations in the Si–Si bond lengths of up to 0.11 Å are found in the substrate, which clearly points to accuracy limitations of semiempirical techniques such as the MNDO/d method in predicting properties of solids and surfaces. The surface Si dimer bond length of the substrate clusters $Si_{13}H_{12}$ and $Si_{15}H_{16}$ prior to benzene adsorption are computed to be 2.26 and 2.27 Å, respectively, in good agreement with the 2.25–2.29 Å predicted by DF slab model calculations on the clean and reconstructed Si(001) surface [28,31]. In the “butterfly” adsorption complex, the formation of a C=C double bond is accompanied by a bond contraction of 0.05 Å with respect to the bond length of benzene in the gas phase, while the C–C single bonds are found to be elongated by 0.11 Å with respect to this reference. The bond angles at the three-fold coordinated carbon atoms of benzene are close to 120°, which indicates almost perfect sp^2 hybridization. Likewise, the bond angles at the four-fold coordinated carbon atoms scatter slightly around the ideal tetrahedron angle of 109.5° associated with sp^3 hybridization. The only bond angle far from these ideal values, i.e. 95.3°, is that between the surface Si dimers and the Si–C bonds (Table 1). It results from the particular geometrical constraint imposed by the Si(001)-(2 × 1) surface. However, the strain which should be associated with such an unusual bond angle is expected to be reduced quite substantially, as is often found in silicon compounds compared to carbon analogues. The Si–C and Si dimer bonds (1.97 and 2.46 Å, respectively) are considerably longer than those typically encountered in organo-silicon compounds [17] or in bulk silicon [14]: $d(SiC)=1.85\text{--}1.88\text{ Å}$ and $d(SiSi)=2.33\text{--}2.35\text{ Å}$.

Table 1

Optimized structure of the “butterfly” and the “pedestal” (in parentheses) adsorption complex $C_6H_6/Si(001)$ obtained from semiempirical MNDO/d and “first principles” LCGTO-DF model cluster calculations

Quantity	LCGTO-DF		MNDO/d	
	$C_6H_6/Si(001)$	$Si(001)C_6H_6$	$C_6H_6/Si(001)$	$Si(001)C_6H_6$
$d(CC)$	1.35	1.40	1.36	1.41
$d(CC_d)$	1.51 (1.47)	1.40	1.53 (1.51)	1.41
$d(C_dC_d)$	(1.58)	1.40	(1.59)	1.41
$\angle(HCC)$	121.4	120.0	123.0	120.0
$\angle(HCC_d)$	119.4 (117.3)	120.0	117.9 (117.1)	120.0
$\angle(H_dC_dC)$	112.8 (111.3)	120.0	112.1 (109.6)	120.0
$\angle(H_dC_dC_d)$	(110.8)	120.0	(110.0)	120.0
$\angle(CCC_d)$	119.2	120.0	118.8	120.0
$\angle(CC_dC)$	109.9	120.0	109.6	120.0
$\angle(CC_dC_d)$	(114.5)	120.0	(115.0)	120.0
$\angle(C_dCC_d)$	(124.8)	120.0	(125.7)	120.0
$d(Si_dC_d)$	1.97 (2.07)		1.94 (1.97)	
$\angle(CC_dSi_d)$	104.8 (111.1)		104.8 (109.5)	
$\angle(C_dC_dSi_d)$	(101.5)		(100.4)	
$\angle(C_dSi_dSi_d)$	95.3 (78.5)		97.4 (79.6)	
$\angle(C_dSi_dSi')$	118.8 (138.8)		112.4 (133.2)	
$\angle(C_dSi_dSi')$	(108.3)		(103.0)	
$d(Si_dSi_d)$	2.46 (2.40)	2.26 (2.27)	2.35 (2.30)	2.23 (2.22)
$d(Si_dSi)$	2.37 (2.40)	2.33 (2.33)	2.28 (2.30)	2.25 (2.24)
$d(Si_dSi')$	(2.34)	(2.33)	(2.25)	(2.24)

In the columns entitled “ $Si(001)C_6H_6$ ”, the computed equilibrium geometries of the individual constituents, the uncovered substrate clusters and a gas-phase benzene molecule are given for comparison. The dimer silicon atoms are denoted by Si_d , the subsurface silicon atoms by Si and Si' , with the latter being the subsurface atom directly below the adsorbate (Fig. 1a). Accordingly, the carbon atoms involved in the $Si-C$ bond and the hydrogen atoms directly bound to them are referred to as C_d and H_d , while C and H denote the sp^2 hybridized carbon atoms and their associated hydrogen atoms. Bond lengths are given in Å, bond angles in degrees.

However, the $Si-Si$ dimer bond, elongated by 0.2 Å, can be regarded as preserved (at least to a significant extent) since it is still substantially shorter than the $Si-Si$ distance of 3.84 Å found for an unrelaxed $Si(001)$ surface and the 1,4-carbon distance of the adsorption complex (about 2.8 Å; see Fig. 1b).

Upon chemisorption, the adsorbate is quite substantially distorted. Furthermore, the aromatic π system of benzene is destroyed, partially in the case of the “butterfly” structure and entirely in case of the “pedestal” structure. Thus, one may ask whether the formation of new $Si-C$ bonds can really compensate for these effects. An instructive way of estimating the energy which is required to “prepare” a benzene molecule for bonding is

to consider the corresponding spin-uncoupled multiplet states of benzene [34]. The adsorbate has to adopt the final adsorption geometry and it has to be promoted into a state where the proper number of dangling bonds is provided at the appropriate sites. To this end, the excitation energies of benzene in the final equilibrium geometries of the two structure models have been calculated using the same basis sets and density functionals as for the “first principles” geometry optimization. The bond-prepared “butterfly” structure of benzene was found to correspond to a triplet HOMO–LUMO $\pi-\pi^*$ excitation 4.5 eV above the gas-phase ground state. A total spin density of 1.6 au was encountered at the 1,4-carbon atoms. For the “pedestal” structure, bond preparation is

achieved by a similar quintet excitation with an overall spin density of 2.9 au on the four bonding carbon atoms and an excitation energy of 9.1 eV. This is twice as much as the energy required to prepare the “butterfly” benzene complex, and thus very nicely demonstrates that, as far as energetics are concerned, the four-fold bound benzene molecule in the “pedestal” structure provides a reasonable alternative to the di- σ bound “butterfly” species. From the experimental heats of formation of alkenes, silanes, and mixed organo-silicon compounds [17,35], the Si–C bond formation energy is estimated to be 3.1 eV. However, one has to take into account that due to geometrical constraints imposed by the Si(001) surface, the formation of the Si–C bonds is not as perfect as in gas-phase molecules (e.g. bonding angles of less than 80° are encountered in the adsorption complexes; Table 1). Since dangling bonds are already present at the clean Si(001)-(2 × 1) surface, the substrate is almost bond-prepared from the very beginning. Thus, the energies for Si–C bond formation for spin-uncoupling and distortion of the constituents of the adsorption complex are estimated to cancel each other to a large extent in the adsorption complex C₆H₆/Si(001). Therefore, quantum chemical calculations on the entire adsorption complex are necessary to ultimately determine the energetically preferred structure.

3.2. The electronic structure

As demonstrated in a series of investigations on the adsorption of hydrocarbons at transition-metal surfaces [24–26], Kohn–Sham one-particle energy spectra can provide qualitative and even semiquantitative information on photoemission (and inverse photoemission) spectra, although rigorously only the highest occupied Kohn–Sham orbital is directly related to the ionization energy of the adsorption system considered. Within that approach, the surface sensitivity of the photoemission signals is generally simulated by an appropriate projection of the electronic states of model systems onto the adsorbate and the top substrate layers. In the present investigation, Mulliken populations of the adsorbate have been used for that purpose. It would have been interesting to include the top

silicon surface layer in order to account for contributions to the photoemission signal which arise from the Si–C and Si–Si dimer bonds. However, because of the rather rich basis sets employed here and the well-known ensuing ambiguities of a population analysis, we would hardly have been able to separate these contributions properly from the remaining Si backbond states to the subsurface layer.

To obtain a direct estimate of the photoemission spectrum of benzene adsorbed on Si(001), and to simultaneously allow for a symmetry classification of the individual peaks, symmetry-resolved projected densities of states (SRPDOS) have been computed according to

$$Q^{(i)}(\epsilon) = \sum_n^{(i)} q_n(ad) e^{-(\epsilon - \epsilon_n)^2/2\sigma^2}, \quad (1)$$

where the Gaussian broadening $\sigma = 0.2$ eV has been chosen in agreement with the experimental resolution [12]. Here, $q_n(ad)$ and ϵ_n are the benzene populations and the one-particle energies, respectively, of the individual Kohn–Sham cluster orbitals. The summation runs over all states of a given irreducible representation Γ_i . In Fig. 2 the resulting symmetry-resolved densities of states of the two C₆H₆/Si(001) model clusters are compared to each other; also shown are the total projected densities of states of the model systems. Several distinct features are discernible in these simulated photoemission spectra.

As discussed in more detail elsewhere [12], the σ system of benzene is essentially maintained upon chemisorption in the “butterfly” configuration, while the delocalized π system of the adsorbate is almost completely destroyed. The same finding holds for chemisorption in the “pedestal” configuration. Those peaks in the simulated spectra of the “butterfly” and the “pedestal” structure which are due to the benzene σ system-derived orbitals of the adsorption complexes can easily be identified (as verified by inspection of the corresponding cluster orbitals). They are labeled according to the associated D_{6h} symmetric orbitals of gas-phase benzene (see Fig. 2). The aromatic π system, on the other hand, partially rearranges into new C=C π bonds or localized electrons, respectively, and partially it is subsumed in the Si–C bonds toward

the substrate. For the “butterfly” structure, two orbitals describing the carbon double bonds of the 1,4-cyclohexadiene-like adsorption complex are expected. They emerge at 6 eV from the simulated photospectrum as symmetric (a_1) and anti-symmetric (b_2) linear combinations of the involved C=C π orbitals (Fig. 2a). For the “pedestal” structure, two sets of properly symmetrized linear combinations of the more or less isolated p_z orbitals (symmetric: a_1 , anti-symmetric: b_1) are expected to occur close to the Fermi level. The occupied levels, holding the two unpaired electrons of the adsorbate, are found at 4 eV. Their unoccupied minority spin partners follow at 2.5 eV (Fig. 2b). However, no particular resonant cluster states could be identified which would have been associated with any of the remaining carbon p_z orbitals or with the Si–C bonds. In contrast, contributions from these orbitals are found to be delocalized rather substantially, energetically as well as spatially. Nevertheless, several small peaks associated with minor adsorbate populations of this type are discernible in the SRPDOS (e.g. the a_1 features around 10 eV or the b_1 signal at 8.3 eV in the spectrum of the “butterfly” structure and the a_2 signal at 6.5 eV in the spectrum of the “pedestal” structure).

For the structure determination of the adsorption complex, we will focus on those parts of the simulated spectra which differ significantly to allow a discrimination between the two structure models. The most striking difference in the SRPDOS of the “butterfly” and the “pedestal” model clusters is the splitting of the formerly degenerate $2e_{2g}$ orbital of benzene (at about 15.5 eV). The energetic order of the a_1 and a_2 orbitals resulting from the chemisorption-induced symmetry reduction to C_{2v} is reversed in the two structure models. To rationalize this finding, the four pertinent adsorbate orbitals are depicted in Fig. 3. At first glance, the orbital pairs of the two structures models look rather similar. However, they differ in the amount of Si–C bond admixture. In the “butterfly” structure the totally symmetric a_1 orbital exhibits some contribution from the two Si–C bonds, while no such admixtures are possible for the a_2 orbital due to its nodal structure. For the “pedestal” structure,

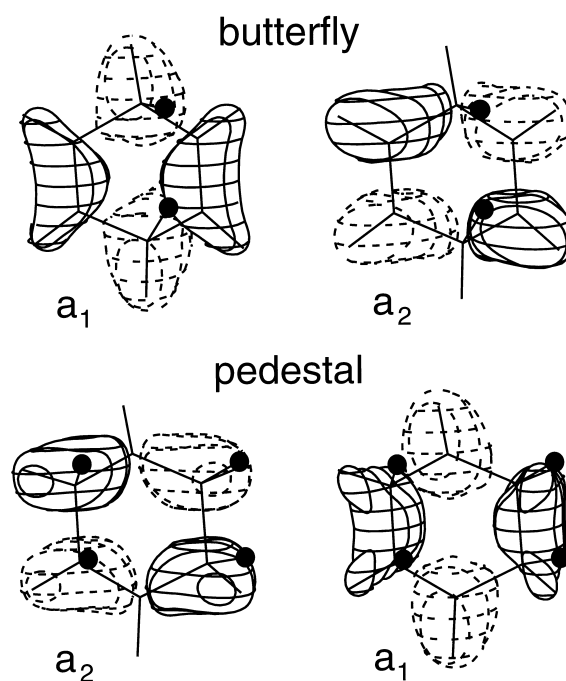


Fig. 3. Shape of the a_1 and a_2 orbitals of the “butterfly” and the “pedestal” model clusters which result from the $2e_{2g}$ state of the adsorbate, viewed approximately along the (001) direction. The positions of the surface dimer silicon atoms participating in the Si–C bonds are marked by filled circles. The orbitals with the higher Kohn–Sham energy are displayed on the left-hand side of the figure, those with the lower energy on the right-hand side.

the opposite situation is encountered: the a_2 orbital features contributions from the four Si–C bonds, while the Si–C bonds happen to fall approximately into the nodal surfaces of the a_1 orbital, thus preventing any significant admixtures of Si–C σ -orbitals (see Fig. 3). Because the silicon dangling bond states subsumed in the Si–C bonds are considerably higher in energy than the benzene $2e_{2g}$ orbitals, bonding Si–C admixtures to the benzene orbitals will occur wherever possible. Accompanied by the corresponding energetic stabilization, this leads directly to the opposite ordering of the benzene-derived a_1 and a_2 levels predicted by the two model clusters (see Fig. 2). A similar energetic interchange of orbitals is calculated for the symmetry-split partners of the benzene $3e_{2g}$ orbital set close to 8.5 eV. All other features of the simulated photoemission spectra below 7 eV

are quite similar for the two structure models. Being aware of the limitations of the present simulation approach to the photoemission spectrum of the $C_6H_6/Si(001)$ adsorption system, we refrain from extracting further information from the more subtle differences in the computed SRPDOS.

From the analysis of the angular dependence of the photoemission signals, it has been deduced [12] that the more strongly bound orbital ($E_b=14.1$ eV) belongs to the totally symmetric representation of the symmetry group C_{2v} , while the more weakly bound orbital (12.9 eV) has pure a_2 character. The same energetic ordering is found for the benzene $3e_{2g}$ -derived orbitals: an a_1 level at 6.5 eV and a more weakly bound a_2 level at 5.7 eV. This experimentally observed sequence of the formerly degenerate states coincides precisely with the splitting pattern calculated for the “butterfly” structure (Fig. 2a), but is at variance with the computed ordering for the “pedestal” structure. We therefore conclude from this comparison of experimental and theoretical photoemission data that benzene is chemisorbed on $Si(001)-(2 \times 1)$ in a 1,4-cyclohexadiene-like structure.

We can even go one step further. The benzene $2e_{2g}$ -derived split orbital pair of a slightly tilted 1,3-cyclohexene-like adsorption complex (Fig. 1c) would be rather similar to the pair of a_1/a_2 orbitals shown in Fig. 3. In that case, they are discriminated according to their even/odd character with respect to the reflection plane through the Si dimers. Thus, the rationalization for the different energetic ordering given above also holds approximately for such a one-sided bound adsorption complex. The a_2 -type (odd) partner would acquire a larger Si–C bonding admixture, thus resulting in the same experimentally excluded splitting pattern as found for the “pedestal” structure.

Not only the computed splitting pattern of the benzene $2e_{2g}$ - and $3e_{2g}$ -derived orbitals matches the experimental observation. The SRPDOS of the “butterfly” structure as a whole agrees quite well with the measured photoemission spectrum if one takes into account the well-known tendency of Kohn–Sham one-particle energy differences to underestimate the corresponding differences of

experimental valence ionization energies. This comparison is carried out in more detail elsewhere [12]. Perfect agreement in the assignment of the photoemission peaks and their symmetry character is achieved for the adsorbate-induced features up to the bottom region of the valence band of silicon (i.e. up to the $2b_{1u}$ -derived level). The same holds for the upper part of the photoemission spectrum starting from the $3e_{2g}$ -derived state, although the analysis of the experimental data in that energy range is complicated by the presence of substrate related features such as dangling-bond states and the surface Si dimer resonance [12]. Between 10 and 11 eV, the assignment of symmetry character to the individual photoemission peaks is less stringent.

3.3. The vibrational structure

Further information about the structure of the adsorption system $C_6H_6/Si(001)-(2 \times 1)$ may be gleaned from the vibrational properties of the adsorption complex. Thus, the vibrational modes of the two model clusters have been computed at their equilibrium structures, at both the semiempirical and “first principles” levels of theory. As for the geometry optimization, only the internal structure of the adsorbate, its location relative to the $Si(001)$ surface and the position of the surface dimer silicon atoms are included in the vibrational analysis. All remaining Si (and hydrogen) atoms of the model clusters are kept fixed. The vibrational modes and their frequencies have been calculated by diagonalizing the mass-weighted force constant matrix as obtained from finite differences to analytical forces. For the DF calculations the vibrational analysis was restricted to the totally symmetric modes. In case of the far less demanding MNDO/d calculations, the non-symmetric modes have also been considered.

In Fig. 4 the totally symmetric vibrational modes of the two structure models, “butterfly” and “pedestal”, as resulting from the DF cluster calculations are compared to each other. Inspection of the individual vibrational modes reveals that only the modes at the low- and high-energy sides of the spectrum can be approximately associated with vibrations of certain internal modes such as frus-

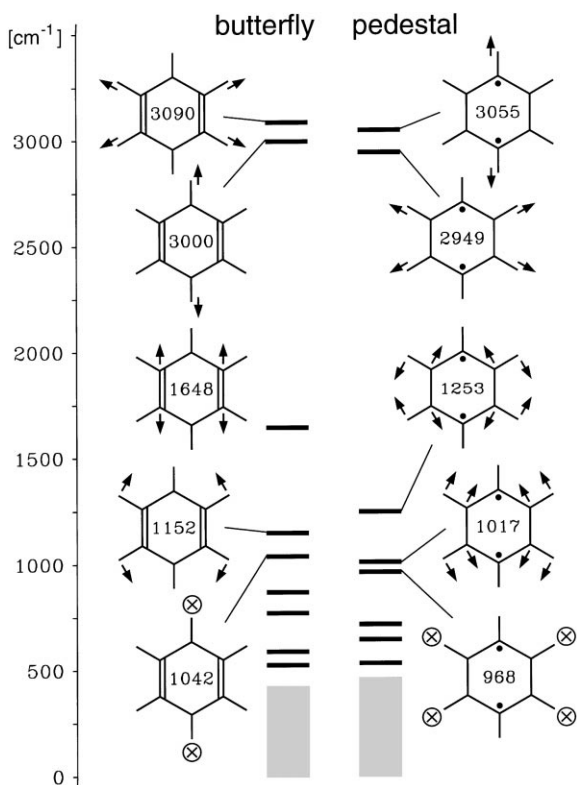


Fig. 4. Comparison of the totally symmetric vibrational modes of the “butterfly” and “pedestal” model cluster calculated with the LCGTO-DF method. The substrate dominated vibrational modes (below 500 cm^{-1}) are indicated as shaded boxes. The characteristics of the uppermost five vibrational modes of each structure model are shown schematically on the left- and right-hand sides of the figure. Also given are the corresponding frequencies (in cm^{-1}). In-plane movements are marked by arrows, out-of-plane movements by \otimes .

trated translation or C–H stretching. In the intermediate energy range strong coupling of the bond coordinates occurs, which makes it difficult or even impossible to assign any simple classification to these vibrational modes.

Here, we will focus on the vibrations with frequencies above 550 cm^{-1} because so far, experimental data on the vibrational structure of benzene adsorbed on Si(001)-(2×1) are only available for that energy range [9]. To facilitate the assignment, the character of the five uppermost totally symmetric vibrational modes of the two structure models shown in Fig. 4 are indicated schematically. As

expected, the spectrum of the totally symmetric vibrational modes features two C–H stretching modes at the high-energy side, at about 3000 and 3100 cm^{-1} (MNDO/d: 3250 and 3400 cm^{-1}). In case of the “butterfly” structure, these C–H stretching modes are followed by the totally symmetric C=C double-bond stretching mode at 1648 cm^{-1} and an in-plane C–H bending mode of the hydrogen atoms bound to the sp^2 carbon atoms at 1152 cm^{-1} . In the “pedestal” structure the corresponding carbon atoms participate in the Si–C bonds and thus only C–C single bonds remain. Two mixed C–C stretching/C–H in-plane bending modes at 1253 and 1017 cm^{-1} are found here. These in-plane modes are followed by the first (totally) symmetric out-of-plane bending mode, at 968 cm^{-1} in the “pedestal” structure and at 1042 cm^{-1} in the “butterfly” structure. Substrate silicon atoms are found to become significantly involved in the vibrational modes of the adsorption complex for frequencies below 500 cm^{-1} only. However, some minor silicon admixtures (less than 20%) occur in the vibrational modes at 593 and 528 cm^{-1} of the “butterfly” structure.

Undoubtedly, the isolated 1648 cm^{-1} mode (MNDO/d: 1745 cm^{-1}) of the “butterfly” structure which is completely missing in the spectrum of the “pedestal” structure is the most striking difference between the two structure models. This continues to hold even when the non-symmetric modes are also considered. The anti-symmetric b_2 partner of the C=C stretching mode of the “butterfly” structure is found only 25 cm^{-1} lower in energy in the semiempirical vibrational analysis, while the next lower vibrational frequency (a b_1 mode) is far away at 1412 cm^{-1} and the first vibrational mode of the “pedestal” structure which follows the high-energy C–H stretching modes in the MNDO/d calculations is a b_2 mode with a frequency of 1453 cm^{-1} .

There is yet another interesting difference predicted between the two structure models concerning the intensity distribution of the C–H stretching modes. For both structures, the totally symmetric C–H stretching modes are split into one which involves only the 1,4-carbon bound hydrogen atoms, and another which exclusively includes the

remaining four hydrogen atoms (see Fig. 4). As revealed by the semiempirical vibrational analysis, the same partitioning also holds for the non-symmetric C–H stretching modes; their frequencies are found to scatter by less than 12 cm^{-1} around the frequencies of the corresponding totally symmetric modes. Thus, two well-separated groups of C–H stretching mode frequencies are expected to occur in the vibrational spectrum of benzene on Si(001). In both structures, the C–H stretching modes at the four-fold coordinated carbon atoms exhibit the lower frequency (Fig. 4), in agreement with the generally accepted rule of thumb [1] that C–H stretching modes of hydrogens bound to sp^3 -hybridized carbon atoms are somewhat lower in energy ($\sim 3000\text{ cm}^{-1}$) than those of sp^2 -hybridized carbon bound H atoms ($\sim 3100\text{ cm}^{-1}$). Therefore, taking into account an EELS resolution of 65 cm^{-1} as achieved by Taguchi et al. [9], a double peak with a 2:1 intensity distribution is expected for the two structure models at about 3000 cm^{-1} , skewed to the high-energy side in the case of the “butterfly” structure and to the low-energy side in the case of the “pedestal” structure, simply because of the different number of oscillators participating in the two kinds of stretching modes.

Experimentally, there exists an isolated loss peak at 1635 cm^{-1} in the EELS spectra of C_6H_6 chemisorbed on Si(001)-(2 × 1) [9] (and a corresponding peak at 1595 cm^{-1} for the deuterated benzene species), a feature which has been attributed to a C=C double-bond stretching mode [9]. Such a vibrational frequency is only discernible in the calculated phonon spectrum of the “butterfly” structure (Fig. 4). Moreover, the intensity of the C–H stretching modes at 3065 cm^{-1} (2300 cm^{-1} for C_6D_6) is much higher than the intensity of the low-energy C–H stretching modes at 2935 cm^{-1} (2190 cm^{-1} for C_6D_6). Again, this experimental observation uniquely matches the intensity distribution predicted for the “butterfly” structure (see above). Hence, from the calculated vibrational properties of the adsorption complex, a “butterfly” structure as shown in Fig. 1b is deduced for benzene on Si(001).

According to Taguchi et al. [9], all but the lowest two EELS peaks are dominated by impact

scattering. No dipole selection rules apply in this case, and thus totally symmetric as well as non-symmetric vibrational modes should be recorded in the energy-loss spectra. Yet, there is a remarkable agreement between the EELS spectra and the frequencies computed for the totally symmetric vibrational modes alone, both for benzene and deuterated benzene (see Table 2). Except for the small shoulder observed at 1080 cm^{-1} in the EELS spectrum of deuterated benzene, there is a one-to-one correspondence between the loss peaks for C_6H_6 as well as for C_6D_6 and the corresponding totally symmetric vibrational modes calculated for the “butterfly” model cluster, as shown in Table 2. The origin of the 1080 cm^{-1} mode for C_6D_6 is unclear, but an assignment to a non-symmetric vibrational modes is suggested.

Isotope shifts are an experimental tool to gain additional insight into the character of individual vibrational modes. Such an analysis is useful under the condition that the constitution of the modes does not change too much upon deuteration. As

Table 2

Harmonic frequencies ν_{DFT} of the totally symmetric vibrational modes of the “butterfly” model cluster for the $\text{C}_6\text{H}_6/\text{Si}(001)$ adsorption complex (Fig. 1b) as computed with the LCGTO-DF method in comparison to experimental values ν_{exp} obtained from EELS measurements [9]

ν_{DFT}		$E_{\text{kin}}(\text{H/D})$		ν_{exp}	
C_6H_6	C_6D_6	C_6H_6	C_6D_6	C_6H_6	C_6D_6
528	493	16	22		
593	552	21	21	615	550
774	650	52	60	790	660 ^a
873	885	17	20	910	860 ^a
1042	754	80	64	1075	785 ^a
1152	853	92	76	1170	860
					1080 ^a
1648	1610	7	9	1635	1595
3000	2216	92	83	2935	2190
3090	2304	91	78	3065	2300

Columns entitled C_6H_6 refer to benzene, columns entitled C_6D_6 to deuterated benzene, each adsorbed on Si(001). The central columns show the percentage of kinetic energy E_{kin} (H/D) attribute to the hydrogen/deuterium motion within each calculated vibrational mode. Vibrational frequencies are given in cm^{-1} . Vibrational modes with similar characteristics are gathered by rows.

^aThe assignment differs from that proposed in Ref. [9]

an example, we have examined the isotope effects on the vibrational modes of the “butterfly” adsorption complex (Table 2). We use the fraction of the kinetic energy associated with the motion of the hydrogen (or deuterium) atoms to quantify the contribution of these atoms to each vibrational mode (see Table 2). As expected, the vibrational modes near 3000 cm^{-1} and at $1152\text{--}1042\text{ cm}^{-1}$ which have already been identified as C–H stretching and C–H bending modes (Fig. 4) exhibit the highest hydrogen/deuterium contribution and consequently the largest isotope shifts. On the other hand, the frequency of the C=C stretching mode at 1648 cm^{-1} is predicted to decrease by only 38 cm^{-1} , in line with its minor hydrogen/deuterium contribution of 7–9%. Clearly, the constitutions of the individual vibrational modes change rather substantially upon deuteration (up to 20%), yet the main character of vibrational modes above $\sim 500\text{ cm}^{-1}$ is maintained (Table 2). This should permit a facile identification of the EELS peaks based on experimentally observed isotope shifts.

Using our calculated data, we are not able to fully confirm the assignment of the EELS signals proposed by Taguchi et al. [9]. The loss signal at 1075 cm^{-1} (785 cm^{-1} for C_6D_6) which has been attributed to an in-plane C–H bending mode [9] is, according to our DF calculations, due to a totally symmetric out-of-plane C–H bending mode. Furthermore, the EELS signal at 910 cm^{-1} was interpreted as another in-plane C–H bending mode associated with a significant isotope shift down to 660 cm^{-1} . However, according to our analysis, the 910 cm^{-1} signal corresponds to a benzene C–C breathing mode with only a minor (reverse) isotope shift from 873 up to 885 cm^{-1} . The corresponding mode of the deuterated adsorbate complex is found to be degenerate (within the experimental resolution) with the C–D in-plane bending mode calculated at 853 cm^{-1} (Table 2), and is actually observed at 860 cm^{-1} [9]. Because of this accidental degeneracy, the experimental association of related C_6H_6 and C_6D_6 modes as assumed by Taguchi et al. [9] does not seem to hold for frequencies below 900 cm^{-1} . According to the DF results, the EELS peak at 790 cm^{-1} is related to the 660 cm^{-1} signal of the deuterated

adsorbate rather than the one at 550 cm^{-1} . This assignment results in a much smaller $v_{\text{H}}/v_{\text{D}}$ ratio of 1.20 (instead of 1.44), in agreement with the non-negligible carbon contribution calculated for this vibrational mode (which is a kind of benzene wagging motion). High-resolution EELS measurements of benzene adsorbed on a one-domain Si(001)-(2 × 1) surface with a low defect concentration are necessary to clarify this point and to address the more subtle vibrational properties of $\text{C}_6\text{H}_6/\text{Si}(001)$ in the low-energy range.

3.4. The (2 × 1) LEED pattern

As already mentioned, a (2 × 1) LEED pattern is observed for the $\text{C}_6\text{H}_6/\text{Si}(001)$ adsorption system at saturation coverage [9,12], although temperature desorption analysis [9] yields a benzene coverage of only 0.27 ML. For $\text{C}_6\text{H}_6/\text{Si}(001)$ adsorption with flat-lying benzene, as deduced from recent angle-resolved photoemission spectra [12], a saturation coverage of a quarter layer is reasonable, simply because of the steric requirements of the adsorbed benzene molecules. The occurrence of a (2 × 1) LEED pattern is therefore not evident at first glance. Well-ordered adsorbate layers with a 1/4 ML coverage should yield surface unit cells such as (2 × 2) or c(4 × 2) which are at least four times larger than the ideal unit cell of bulk-terminated Si(001). On the other hand, there is no reason to assume electron diffraction to be insensitive to the adsorbate layer in the present case of benzene chemisorbed on Si(001).

To resolve this problem, one can start from the basic assumption underlying the present work (see Section 2) that benzene adsorbs on top of the dimer rows of the reconstructed Si(001)-(2 × 1) surface. Regular ordered chains along these rows are to be expected because of the necessity of binding to the dangling bonds of the well-ordered surface dimers. However, since these chains are separated by 7.68 \AA perpendicular to the dimer rows, inter-chain interaction hardly exists even at saturation coverage. No substantial energy difference is therefore expected between a (2 × 2)-like alignment of neighboring adsorbate chains with

benzene molecules located on surface dimers in registry between two dimer rows, and the alternative $c(4 \times 2)$ -like alignment with neighboring benzene chains shifted by one dimer along the rows with respect to their neighboring chains. Thus, there is strong evidence for the adsorption system $C_6H_6/Si(001)$ to consist of one-dimensionally well-ordered but randomly aligned chains of benzene molecules. It is straightforward to show that the structural factor of such a partially ordered adsorbate layer leads to sharp LEED spots at the $(n/2, m)$ positions (corresponding to a (2×1) overlayer), while the half-integer spots along the dimer rows (the y axis) are smeared out into weak homogeneous lines along the x axis in reciprocal space. Taguchi et al. [9] did not find any additional lines in the LEED image of the adsorption system $C_6H_6/Si(001)$. However, a slightly increased background intensity was noticed [9] which might be interpreted as the remnants of the expected streaks.

Although designed for adsorption on top of the surface dimer rows, this rationalization also holds for hypothetical adsorption above the $Si(001)$ - (2×1) troughs. However, there is one important difference: if benzene was adsorbed above the troughs, isolated surface Si atoms would be created in response to the formation of the Si–C bonds. As long as adsorption takes place in a well-ordered (2×2) fashion, all these surface atoms are finally subsumed in some Si–C bond at saturation coverage. On the other hand, randomly shifted benzene chains above the troughs or a $c(4 \times 2)$ adsorbate overlayer would leave many of the Si surface atoms unsaturated. If this latter situation is ruled out as being energetically disfavored, the fact that no such (2×2) LEED pattern is observed experimentally may be regarded as further independent evidence for the adsorption of benzene on $Si(001)$ to occur on top of the dimer rows.

4. Summary

Based on the available experimental data for benzene adsorbed on $Si(001)$ [9,12], and also by taking into account the results of semiempirical geometry optimizations on that adsorption system

[10,11], two structure models for $C_6H_6/Si(001)$ have been proposed. Both meet the most important experimental observations: local C_{2v} symmetry and di- σ bonding towards the Si surface. Furthermore, only adsorption on top of the $Si(2 \times 1)$ surface dimer rows has been considered because the creation of energetically disfavored unsaturated isolated surface Si atoms is avoided in this way.

In agreement with previous studies [10,11], the “pedestal” structure with a four-fold bound benzene species (Fig. 1a) was found to be more stable by about 1.0 eV at the semiempirical level of theory. However, using a “first principles” density functional approach, the energetic ordering is reversed, and the 1,4-cyclohexadiene-like “butterfly” structure (Fig. 1b) becomes energetically favored by 1.4 eV.

To support this result and to arrive at a definite assignment of the structure of the adsorption complex, the electronic and vibrational structure has been calculated for both structure models. Several distinct differences were identified between the “butterfly” and the “pedestal” structures. The energetic ordering of adsorbate states which emerges from the formerly degenerate benzene $2e_{2g}$ and $3e_{2g}$ orbitals is different, as can be rationalized by considering the particular nodal patterns of these orbitals and the resulting different amounts of possible Si–C orbital admixtures. The vibrational spectra of the two structure models also exhibit several discriminating features. Most important is a vibrational mode which is related to C=C double bonds; it is measured at about 1635 cm^{-1} and calculated at 1648 cm^{-1} for the “butterfly” structure, but is absent in the spectrum of the “pedestal” structure. In addition, the measured intensity pattern of the two-fold split C–H stretching modes is only compatible with the computational results of the “butterfly” structure. Both discriminating effects are found to be directly related to structural differences in the adsorbate–substrate bonding.

From a comparison of the simulated surface-sensitive photoemission spectra and the vibrational spectra of the two structure models with the experimental data [9,12], it is evident that benzene forms an adsorption complex of local C_{2v} symmetry with

one Si surface dimer in a 1,4-cyclohexadiene-like fashion and with the adsorbate plane parallel to the surface. As expected, C=C double bonds are calculated to contract and C–C single bonds to elongate with respect to the C–C distance in gas-phase benzene. The bond angles at the four- and three-fold coordinated carbon atoms are rather close to the ideal sp^2 and sp^3 hybridization angles (Table 1).

Based on detailed information calculated for the “butterfly” structure model, the assignment of the EELS spectra proposed by Taguchi et al. [9] is somewhat modified. For the deuterated adsorbate, an accidental near-degeneracy of the benzene breathing mode and one of the in-plane bending modes is found. This prevented the correct assignment of C_6H_6 and C_6D_6 modes below 900 cm^{-1} in Ref. [9].

Moreover, a consistent rationalization for the unexpected (2×1) LEED pattern found for benzene on Si(001) at saturation coverage [9] is proposed. While benzene adsorption takes place in a regular fashion along the dimer rows of the Si(001) surface by forming chains of benzene molecules bound to every other Si dimer, these chains are very likely randomly registered relative to each other, resulting in a phase with one-dimensional disordering perpendicular to the Si(001) rows.

Acknowledgements

We thank L.G.M. Pettersson and A. Voityuk for stimulating discussions. We are also grateful to W. Widdra and co-workers for bringing the adsorption system $C_6H_6/Si(001)$ to our attention, for providing us with their experimental results prior to publication, and for many discussions accompanying this investigation. Financial support by the Deutsche Forschungsgemeinschaft via SFB338 and by the Fonds der Chemischen Industrie is gratefully acknowledged.

References

- [1] M. Nishijima, J. Yoshinobu, H. Tsuda, M. Onchi, Surf. Sci. 192 (1987) 383.
- [2] P.A. Taylor, R.M. Wallace, C.C. Cheng, W.H. Weinberg, M.J. Dresser, W.J. Choyke, J.T. Yates Jr., J. Am. Chem. Soc. 114 (1992) 6754.
- [3] W. Widdra, C. Huang, W.H. Weinberg, Surf. Sci. 329 (1995) 295.
- [4] U. Birkenheuer, U. Gutdeutsch, N. Rösch, A. Fink, S. Gokhale, D. Menzel, P. Trischberger, W. Widdra, J. Chem. Phys., in print.
- [5] R.H. Zhou, P.L. Cao, L.Q. Lee, Phys. Rev. B 47 (1993) 10601.
- [6] B.I. Craig, Surf. Sci. 329 (1995) 293.
- [7] Q. Liu, R. Hoffmann, J. Am. Chem. Soc. 117 (1995) 4082.
- [8] A.J. Fisher, P.E. Blöchl, G.A.D. Briggs, Surf. Sci. 374 (1997) 298.
- [9] Y. Taguchi, M. Fujisawa, T. Takaoka, T. Okada, M. Nishijima, J. Chem. Phys. 95 (1991) 6870.
- [10] B.I. Craig, Surf. Sci. 280 (1993) L279.
- [11] H.D. Jeong, S. Ryu, Y.S. Lee, S. Kim, Surf. Sci. 344 (1995) L1226.
- [12] S. Gokhale, P. Trischberger, D. Menzel, W. Widdra, H. Dröge, H.-P. Steinrück, U. Birkenheuer, U. Gutdeutsch, N. Rösch, J. Chem. Phys. 108 (1998) 5554.
- [13] J.H. Callomon, E. Hirota, T. Iijima, K. Kuchitsu, W.J. Lafferty, Structure Data of Free Polyatomic Molecules, Landolt-Brönstein, New Series, vol.II/15, Springer, Berlin, 1987.
- [14] N.W. Ashcroft, S.D. Mermin, Solid State Physics, Saunders, Philadelphia, 1976, Table 4.3.
- [15] W. Thiel, A.A. Voityuk, Int. J. Quantum Chem. 44 (1992) 807.
- [16] A.A. Voityuk, SIBIQ 2.4. A program for semiempirical calculations, 1991.
- [17] W. Thiel, A.A. Voityuk, J. Mol. Struct. 313 (1994) 141.
- [18] B.I. Dunlap, N. Rösch, Adv. Quantum Chem. 21 (1990) 317.
- [19] A.D. Becke, Phys. Rev. A 38 (1988) 3098.
- [20] J.P. Perdew, Phys. Rev. B 33 (1986) 8822, Phys. Rev. B 34 (1986) 7406.
- [21] A.D. Becke, J. Chem. Phys. 88 (1988) 2547.
- [22] P.M.W. Gill, B.G. Johnson, J.A. Pople, Chem. Phys. Lett. 209 (1993) 506.
- [23] P. Strodel, K.M. Neyman, H. Knözinger, N. Rösch, Chem. Phys. Lett. 240 (1995) 547.
- [24] M. Weinelt, W. Huber, P. Zebisch, H.-P. Steinrück, M. Pabst, N. Rösch, Surf. Sci. 271 (1992) 539.
- [25] M. Weinelt, W. Huber, P. Zebisch, H.-P. Steinrück, P. Ulbricht, U. Birkenheuer, J.C. Boettger, N. Rösch, J. Chem. Phys. 103 (1995) 9709.
- [26] U. Gutdeutsch, U. Birkenheuer, E. Bertel, J. Cramer, J.C. Boettger, N. Rösch, Surf. Sci. 345 (1996) 331.
- [27] H. Jörg, N. Rösch, J.R. Sabin, B.I. Dunlap, Chem. Phys. Lett. 114 (1985) 529.
- [28] J.E. Northrup, Phys. Rev. B 47 (1993) 10032.
- [29] T. Hoshino, M. Hata, S. Oikawa, M. Tsuda, I. Ohdomari, Phys. Rev. B 54 (1996) 11331.
- [30] G. Pacchioni, K.M. Neyman, N. Rösch, J. Electron Spectrosc. Relat. Phenom. 69 (1994) 13.

- [31] P. Krüger, J. Pollmann, *Phys. Rev. Lett.* 74 (1995) 1155.
- [32] P.E.M. Siegbahn, U. Wahlgren, in: E. Shustorovich (Ed.), *Metal–Surface Reaction Energetics*, VCH, New York, 1991, p. 1.
- [33] L. Ackermann, N. Rösch, *J. Chem. Phys.* 100 (1994) 6578.
- [34] L. Triguero, U. Wahlgren, L.G.M. Pettersson, P.E.M. Siegbahn, *Theor. Chim. Acta* 94 (1996) 297.
- [35] R.C. Weast, *Handbook of Chemistry and Physics*, CRC Press, Boca Raton, FL, 1988.